Quantum-size effects on radiative lifetimes and relaxation of excitons in semiconductor nanostructures

J. Bellessa
Groupe de Physique des Solides, CNRS, Universités Pierre et Marie Curie et Denis Diderot, 2 place Jussieu, F-75251 Paris Cedex 05, France

V. Voliotis
Groupe de Physique des Solides, CNRS, Universités Pierre et Marie Curie et Denis Diderot, 2 place Jussieu, F-75251 Paris Cedex 05, France and Université d'Evry-Val d'Essonne, Boulevard François Miterrand, 91025 Evry Cedex, France

R. Grousson
Groupe de Physique des Solides, CNRS, Universités Pierre et Marie Curie et Denis Diderot, 2 place Jussieu, F-75251 Paris Cedex 05, France

X. L. Wang, M. Ogura, and H. Matsuhata
Electrotechnical Laboratory, 1-1-4 Umezono, Tsukuba 305, Japan
(Received 15 May 1998)

A systematic study of exciton dynamics is presented in quantum boxes formed naturally along the axis of a V-shaped quantum wire, by means of *time and spatially resolved resonant* photoluminescence. The dependence of radiative lifetimes and relaxation mechanisms of excitons is determined versus the size of the boxes. The radiative recombination rate varies linearly with the length of the box, showing that the exciton has a coherence volume equal to the volume of the box. In a low excitation regime, emission from excited states has not been observed, which would be a consequence of relaxation bottleneck, but there is clear evidence that relaxation via emission of LA phonons depends strongly on the energy separation between the different quantum box levels. [S0163-1829(98)07839-4]

I. INTRODUCTION

Following the success of semiconductor quantum wells (QW's), which permitted one to study two-dimensional optical and electronic effects due to confinement, many investigations have been carried out in similar quasi-one dimensional quantum wires (QWR's) and zero-dimensional quantum boxes (QB's). Recent improvements in growth techniques allowed the fabrication of high-quality semiconductor nanostructures with good optical properties like QW heterostructures grown on nonplanar substrates,[1–3] or V- and T-shaped QWR's,[4–8] or different III-V quantum dots.[9–12] However, fluctuations of size and/or composition still exist, leading to inhomogeneous broadening in the optical spectra, which hides the intrinsic properties of a single quantum structure. Spatially resolved photoluminescence or microphotoluminescence (μPL) spectroscopy in the domain of diffraction limited optics has recently been developed, and allowed one to study, for example, optical properties of ''natural'' QB's formed by well-width fluctuations in narrow GaAs QW's,[13–16] single quantum dots,[9,11,17] or single QWR's.[18–20]

An important problem that has been investigated theoretically and experimentally is the relaxation of carriers in such semiconductor nanostructures and especially in QB's. The impact is of course important concerning the efficiency of optoelectronic devices. It has been predicted that electronic relaxation is quenched whenever the energy separation between levels does not exactly match the energy of a LO phonon, or exceeds a few meV for emission via LA phonons.[21,22] In that case, a strong decrease of photoluminescence (PL) signal should occur. In fact, this predicted relaxation bottleneck remains controversial, and the experimental facts are to our knowledge not completely conclusive. Indeed, in the case of low excitation regime several groups reported on rapid carrier relaxation in different QB systems,[23–25] and only under high pump power has excitation emission from excited states been observed because of state-filling effects.[10,26–29] In order to explain efficient relaxation, mechanisms like multiphonon-assisted emission[30,31] or Auger-like scattering inside one electron-hole pair have been proposed.[32]

Another interesting aspect of quantum confinement in nanostructures is whether the correlated electron-hole pair keeps or loses its excitonic nature. Obviously the answer to the question is related to the size of confinement compared to the exciton Bohr radius, i.e., to the comparison between the kinetic energy and the Coulomb interaction. The density of carriers present in the structure should also change the nature of electron-hole pairs. Nevertheless, this problem is beyond the scope of this work, and hereafter we will call an exciton a correlated electron-hole pair in a general manner.

In this paper we propose to investigate radiative lifetimes and relaxation mechanisms of excitons present in a single QWR by means of *resonant time-resolved* μPL. Recently, μPL experiments have shown that, in QWR's, excitons are

localized at low temperature in local potential minima.[18–20] These potential minima can be viewed as naturally formed QB's with a weak confining potential along the wire axis, since they are formed by one-monolayer (1-ML) thickness fluctuations of the wire. Therefore we expect that exciton relaxation is mainly governed by the dynamical properties of carriers in a zero-dimensional QB. Moreover, microphotoluminescence excitation (μPLE) spectroscopy[33] has revealed that one QWR is segmented into extended sections of hundreds of nm with slightly different confining potentials, and inside these sections the QB's are present. In this way, two systems can be studied in such a structure: the already mentioned QB's and the long sections which can be considered as quasi-one-dimensional QWR's. The μPLE spectra allow us to pump resonantly excited levels of a given QB.[34] Then the resonant time-resolved μPL give the possibility to measure (i) the relaxation times between levels by studying the rise time of the temporal spectrum, and (ii) the radiative lifetime of an exciton in a QB. The measured radiative lifetimes of localized excitons are long compared to the values in a two-dimensional QW, ranging between 300 and 500 ps depending on the QB length along the wire axis. This is, to our knowledge, the first time that the dependence of exciton radiative recombination in a single QB is studied experimentally as a function of the QB size. In some experiments where the μPL of one QWR section is observed, the related QWR exciton radiative lifetime is shorter, about 150 ps. The measured rise times vary from a few ps (which is the experimental time resolution) to 100 ps, and this dispersion of values gives us information about the relaxation mechanisms between the QB levels. Since the confinement energy in the QB's is only a few meV, relaxation is made possible by emission of LA phonons. Emission with LO phonons is not discussed here because the GaAs LO-phonon energy is 36 meV. A clear dependence of relaxation times with the energy separation between the levels is observed as predicted theoretically,[30,35] and the emission rate with a single LA phonon decreases as soon as the energy separation of levels exceeds a few meV.[36] For higher excitation energy, multiphonon emission remains a very efficient relaxation process. All the presented results are performed at low excitation power where there is only one (or less) electron-hole pair created in one QB. The dependence of the resonant time-resolved μPL with excitation power will be the subject of a future publication.

The paper is organized as follows: in Sec. II, we give some details concerning the growth and structure of samples and the experimental setup. Section III is divided in two parts: after the presentation of the μPL and μPLE experiments, we discuss the results obtained on the radiative lifetimes of localized excitons as a function of the size of the QB's. Finally, relaxation processes in QB's are discussed.

II. EXPERIMENTAL DETAILS

The studied GaAs/$Al_xGa_{1-x}As$ QWR's are grown on a 4.8-μm pitch V-grooved GaAs substrate by flow rate modulation epitaxy, a modified metal-organic vapor-phase-epitaxy growth technique which can be controlled on atomic level.[5] The QWR thickness at the center of the V is about 5 nm, and the Al content in the barriers is 33% for the (001) top facet. In order to enhance the PL signal of the QWR, the (001) flat region and part of the (111) *A* sidewall $Al_xGa_{1-x}As$ barrier layers have been removed by selective wet chemical etching.[5] The lateral size where the electronic wave functions are confined is about 15 nm. The full width at half maximum of the PL line for this sample is 8 meV, and the Stokes shift between the PL and PLE is 4 meV,[37] showing the good optical properties of the sample.

Continuous and time-resolved μPL and μPLE experiments have been performed at 6 K using a mode-locked argon laser pumping synchronously a dye laser (LDS 722). The pulse width is 5 ps, and the repetition rate is 82 MHz. The excitation beam is focused with a microscope objective, and the laser spot diameter is 1 μm. The time-resolved PL signal is analyzed through a double monochromator operating in the subtractive mode, and detected by a time-correlated single-photon-counting system with a time resolution of 40 ps. It can be improved if a deconvolution procedure is used. Then the best time resolution achieved is about 10 ps. The spectral resolution is 200 μeV but in μPLE experiments the resolution is given by the width of the laser line, which is 50 μeV. This explains why usually the μPLE peaks are narrower than the μPL ones.

The excitation power in all the presented experiments is low enough that at most one exciton is created in a QB. The number of created excitons can be estimated from the following relation: $N=(\alpha l P \tau/h\nu)\beta$, where αl represents the absorption probability in the material. A typical value which is usually taken in the literature is $\alpha l = 0.6\%$ in a GaAs quantum well.[38] P is the excitation power, τ is either the radiative lifetime of excitons in a continuous excitation or the repetition rate in a pulsed excitation, and β is the ratio between the illuminated wire surface and the laser spot surface. From this relation, it appears that when the pump power is lower than 100 μW (continuous excitation), there is always less than one electron-hole pair per QB. For pulsed excitation the pump power must be lower than 2.5 μW. This estimation is made assuming that the mean radiative lifetime is about 300 ps, which is consistent with our experimental results and that about ten QB's are present in 1 μm, which corresponds to the number of peaks observed in the μPL spectrum. The factor β is taken equal to 0.05.

III. RESULTS AND DISCUSSION

A typical μPL experiment is shown in Fig. 1. It demonstrates the ability to separate properties of a single QWR or a single QB. All spectra have been recorded at the same position on one wire under similar conditions. In the bottom of the figure is represented a μPL spectrum of the QWR. The usual PL line is split into several sharp peaks, separated by 1 or 2 meV and distributed over 10–15 meV. The line is centered around 1.644 eV. This fine structure of the μPL spectrum strongly depends on the observed QWR, and is also modified when moving the laser spot along one wire. We have attributed these peaks to fundamental exciton states localized in minima of the QWR confining potential.[18,33] They are due to size inhomogeneities created by 1-ML thickness fluctuations on the top (001) interface. The confinement energies of the localized states are distributed over 10 meV, and this reflects the size distribution of the QB's, which is

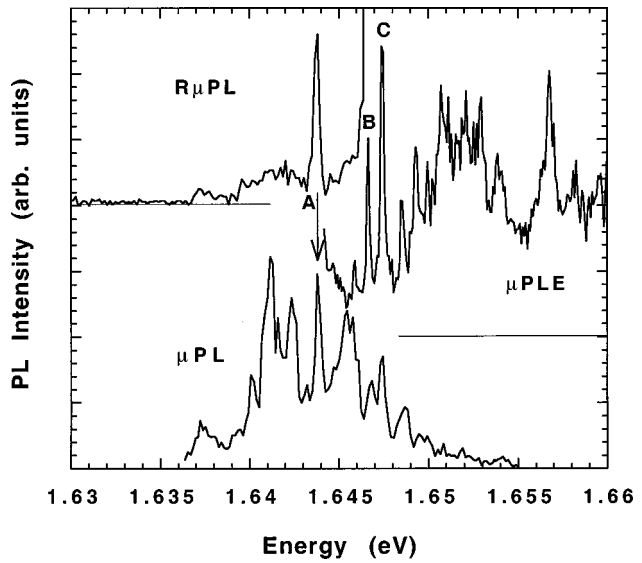

FIG. 1. MicroPL, μPLE and $R\mu$PL. The excitation power is equal to 3 μW. Position A (1.6436 eV) is the detection energy of the μPLE spectrum, and B (1.6464 eV) is the excitation energy of the $R\mu$PL spectrum. Position C is equal to 1.6474 eV.

the origin of the inhomogeneous broadening of the PL line.

In the central part of Fig. 1 is presented a μPLE spectrum detected at 1.6436 eV on a sharp peak of the μPL spectrum labeled *A*. At the energy position of the first e_1-h_1 QWR exciton transition, several peaks as narrow as 0.2 meV are observed. The μPLE peaks are attributed to excited states of the emitting QB and to QWR states corresponding to wire sections with slightly different confining potentials, due to size inhomogeneities along the wire axis.[33] The first peak labeled *B*, and the peak labeled *C*, at 2.8 and 3.8 meV above the detection, are attributed to the first and second excited states of the same QB, respectively. The higher-energy peaks correspond to wire states. From the energy difference between the fundamental (peak *A*) and the first and second excited states (peak *B* and *C*), we can estimate the QB length. Assuming that its potential is 1-ML deep (corresponding to 9 meV) then the length of the QB is about 55 nm. It is worth noting that the μPLE peaks appear at different energy positions when changing the detection energy, because each emitting QB is associated with a different wire section or with several wire sections.

On top of Fig. 1 is presented the resonant μPL ($R\mu$PL) spectrum excited at the energy position of peak *B* (1.6467 eV). Only one peak is observed at 1.6436 eV, which is the energy of peak *A*. This result nicely proves that peaks *A* and *B* are related to the same QB and can be assigned to the QB fundamental and the first excited state, respectively. It is now possible to perform resonant time-resolved μPL in order to analyze the relaxation mechanisms between levels of a single QB or a QWR section, and measure the radiative lifetime of one exciton confined in such a quantum structure.

A. Radiative lifetimes

Figure 2(a) shows the μPL and μPLE spectra corresponding to the resonant time-resolved μPL depicted in Fig. 2(b). The μPLE spectrum has been recorded by detecting on the lowest-energy side peak (indicated by an arrow in the figure).

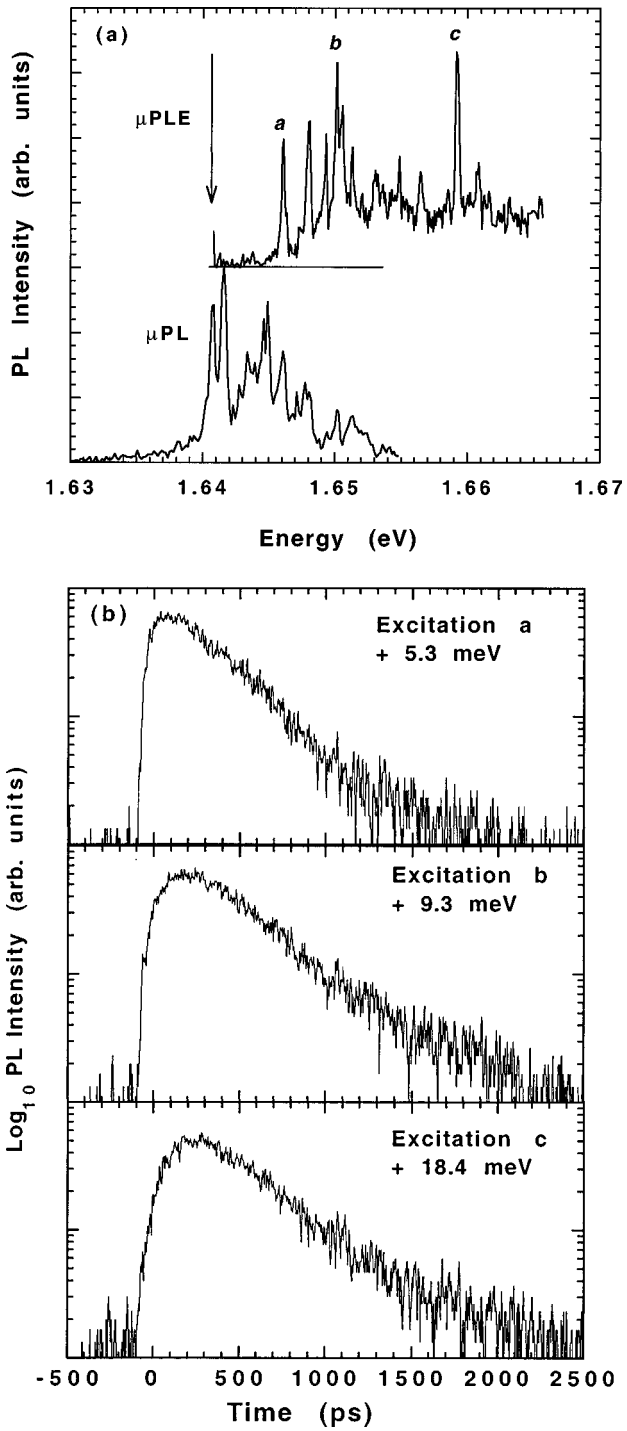

FIG. 2. (a) μPL and μPLE detected on the lowest-energy side peak (1.6408 eV) of the μPL. The detection is labeled by an arrow. Peak positions *a*, *b*, and *c* correspond to the three resonant excitation energies of the time-resolved μPL experiments represented in (b). The pump power for all experiments in (a) and (b) is a few μW.

We have performed resonant excitation of the μPL on peaks labeled *a*, *b*, and *c* on the curve, at 5.3, 9.3, and 18.4 meV, respectively. Peak *a* is attributed to the first excited state of the emitting QB, and peaks *b* and *c* are attributed to the e_1-h_1 and e_1-h_2 transitions of the QWR, respectively. This latter transition is actually forbidden, but it might become allowed because of the asymmetry of the QWR potential. We estimate the QB length to be about 40 nm.

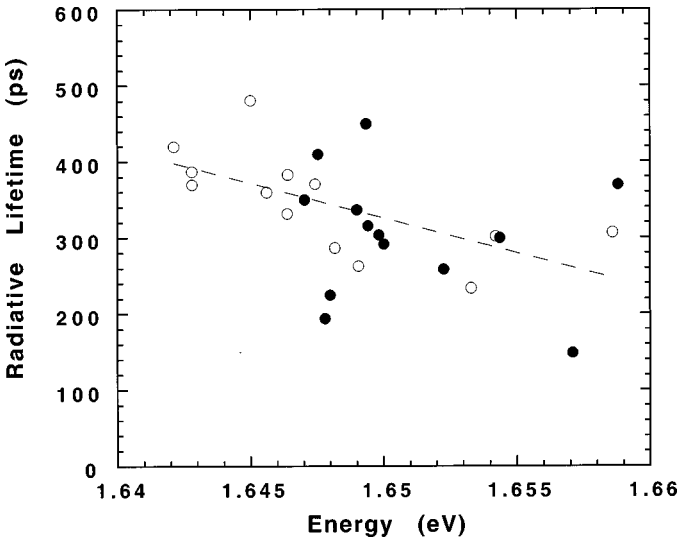

FIG. 3. Measured radiative lifetimes as a function of the energy position in the μPL line. The open and solid symbols correspond to nonresonant and resonant excitation, respectively. The dotted line is just a guide to the eye.

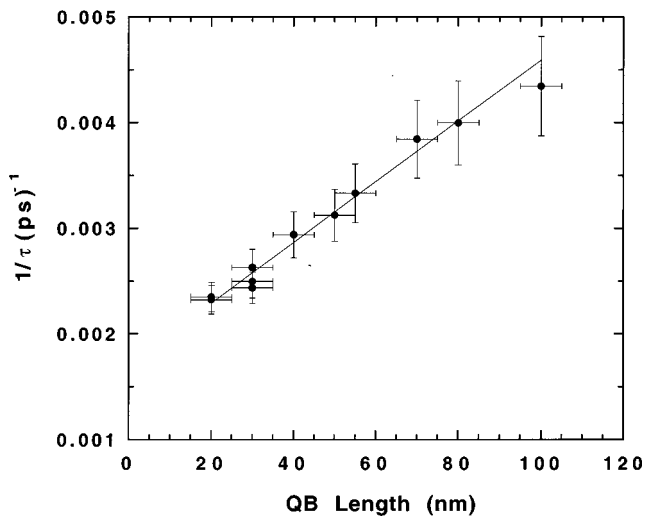

FIG. 4. Radiative recombination rate $1/\tau$, as a function of the QB length L. A linear fit of the experimental data is also shown. The equation of the fit is $1/\tau = aL + b$, with $a = 3.04 \times 10^{-5}$ ($\mathrm{ps}^{-1}\,\mathrm{nm}^{-1}$) and $b = 1.67 \times 10^{-3}$ (ps^{-1}).

The time decay of the $R\mu$PL is quasiexponential for all the excitation energies [Fig. 2(b)]. The three curves can be fitted by the same decay time constant of 350 ps. We can quite safely assume that it represents the exciton radiative lifetime, since the decay time depends neither on the excitation energy nor on the excitation power. We have also checked that the total PL intensity increases linearly as the pump power is increased. This is a good indication that the exciton decay is dominated by radiative recombination. Recent measurements on a single QB but with a different structure give the same order of magnitude for the radiative lifetime of excitons.[24,29] Generally, our experimental results are in agreement with theoretical calculations of exciton radiative lifetimes in QB's,[39,40] but not with the assumption that the radiative lifetime is proportional to the inverse of the homogeneous linewidth of the PL line. Indeed, the μPL peaks are 200 μeV wide. If we assume that the linewidth represents the homogeneous broadening, then we deduce that the phase coherence time (radiative lifetime) should be equal to 2 ps.[41] This means that the lines are broadened by some very fast dephasing mechanism within a few ps, probably related to the electron-hole exchange interaction in the pair, like in two-dimensional structures.[42] Broadening due to thermal energy can be excluded since the kT at 6 K is 0.51 meV, which is larger than the linewidth of the μPL peaks.

For a given μPL spectrum, we can study the emission of several QB's, record for each one the related μPLE spectrum, and perform the time-resolved μPL with a resonant excitation on different excited states of the QB corresponding to the different μPLE peaks. Figure 3 shows the measured radiative lifetimes as a function of the energy position in the μPL, from all the resonant time-resolved experiments. Nonresonant measurements, where the excitation energy lies in the higher energy QWR transitions, are also represented with different symbols on the figure. We observe that the values vary inside the μPL line from 150 up to 500 ps generally increasing as the peak energy position decreases. The dispersion of the experimental values is obviously related to the different QB lengths. Although the peak energy position does not correspond in a straightforward manner to a given variation of the QB length, it appears that the most elongated QB's are related to peaks on the high-energy side of the μPL, since the radiative lifetimes are faster in this energy domain. Indeed this energy range corresponds to the absorption of the first QWR transition, and we expect in this domain to find the most elongated QBs or the QWR-like sections, with faster radiative lifetimes. Citrin[43] calculated that in the case of a GaAs cylindrical QWR (with 10-nm radius) the radiative lifetime of a free exciton is about 150 ps, which is in agreement with our results. Measurements of the temperature dependence of the radiative lifetimes in similar V-shaped QWR's are also in accordance.[44,45]

As we have already discussed, we can deduce, from the energy positions of the μPL and μPLE peaks, the length of the emitting QB. We can then plot, for each time-resolved experiment, the measured radiative lifetime as a function of the QB length. These results are shown in Fig. 4, where the radiative recombination rate $1/\tau$ is plotted versus the length L of the QB. We observe that, as L decreases, the recombination rate decreases linearly. Our results are consistent with theoretical predictions[46–48] made in order to explain the ''giant oscillator strength'' of bulk excitons bound to impurities. Commonly, the radiative recombination rate is related to the oscillator strength according to[49]

$$\frac{1}{\tau} = \frac{ne^2\omega^2}{2\pi\varepsilon_0 m_0 c^3} f, \tag{1}$$

where f is the total oscillator strength (OS) of the transition overall the polarization contributions, and the other symbols are the usual physical constants. For excitonic absorption, the optical matrix element is nonzero only for ns states of the exciton with a wave vector almost equal to zero. Then the OS of the free bulk $1s$ exciton state is equal to

$$f = \frac{2P_{cv}^2}{m_0\hbar\omega}\frac{V}{(\pi a_B^3)} = f_0\frac{V}{(\pi a_B^3)}, \tag{2}$$

where P_{cv}^2 is the dipole matrix element connecting Bloch states in the valence and conduction bands, $\hbar\omega$ is the energy of the transition, a_B the three-dimensional (3D) Bohr radius of the exciton, and V is the volume of the crystal. It appears that the OS is proportional to the ratio of the volume of the crystal to the exciton volume. The OS for a bound exciton can be derived from this last expression by replacing the volume of the whole crystal by the volume within the electron and the hole overlap, i.e., corresponding to the number of cells covered by the center-of-mass motion of the bound exciton. This volume is often called the ''coherence volume'' of the exciton,[35,50] Then the radiative recombination rate scales like

$$\frac{1}{\tau} \propto \frac{V_{\text{coherence}}}{V_{\text{exciton}}(L)}. \tag{3}$$

Under these considerations, when the coherence volume is reduced, the OS is reduced, leading to an increase of the radiative lifetime. In this sense, the situation of an exciton localized in a QB is similar to the 3D bound exciton. As the size of the box is reduced, the coherence volume of the exciton is reduced leading to a decrease of the OS and to a longer radiative lifetime. This effect has been observed a few years ago in CuCl microcrystals.[51] This is also confirmed by our experimental observations, that suggest taking as the coherence volume the volume of the box in which the exciton is confined ($V_{\text{coherence}}=5\times15\times L$ nm^3). It is interesting to notice that in the limit of long boxes where $L \gg a_B$, the experimental data seem to deviate from the linear dependence of the radiative recombination rate with L. Above a coherence length of about 100 nm, they saturate to the value of the exciton radiative lifetime in the QWR. In the studied range of lengths, we have not observed any dependence of the exciton volume, V_{exciton}, with L. In the opposite limit of small boxes where $L<a_B$, the description in terms of coherence volume is no more valid since the center of mass and the relative motion of the exciton are coupled.[52] The determinant factor acting on $1/\tau$ is the volume of the exciton, which for $L \ll a_B$ should vary rapidly with L. Although there is a lack of experimental data, we could expect that in this limit the radiative recombination rate should increase as the size of the QB becomes smaller than a_B, due to an enhancement of the excitonic OS. This would be similar to what was observed in narrow GaAs/$Ga_{1-x}Al_xAs$ QW's.[53] Recent measurements of exciton binding energies in $In_xGa_{1-x}As$/GaAs QB's show that as the size of the boxes is reduced ($L<50$ nm) an important increase of the binding energy is observed.[54] Then the OS should also increase leading to an enhancement of the radiative recombination rate. However, we do not believe that this effect should be so important in the present case, since the confinement energy is only 9 meV.

B. Relaxation processes

As we have already mentioned, resonant excitation on the μPLE peaks permits the determination of the relaxation time between two discrete levels from the measurement of the rise time of the temporal spectrum. The time-resolved spectra are fitted assuming a three-levels model, and deconvoluted by the 40-ps temporal response of the experimental setup.

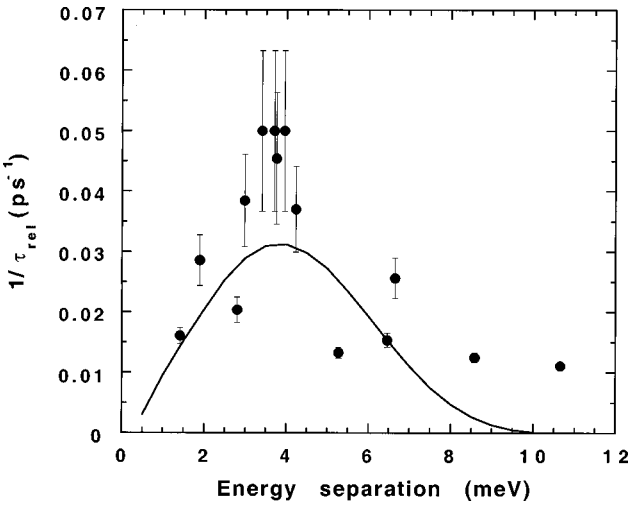

FIG. 5. Relaxation rate $1/\tau_{\text{rel}}$, for different QB's as a function of the energy separation between the excitation (first excited level) and detection energy position (fundamental state). The full line represents the calculated electron–LA-phonon scattering rate from the first excited level to the fundamental state.

Due to the weak confinement in the QB's, the main mechanism responsible for relaxation between quantum levels is emission of LA phonons. The PL is then efficient only when the separation in energy between levels does not exceed a few meV. From energy and momentum conservation arguments,[36] we can deduce the maximum phonon energy leading to significant scattering rates and given by the simple relation

$$E_{\max}=\hbar c_s q_{\max} \approx \frac{hc_s}{L_z}, \tag{4}$$

where c_s is the sound velocity in the material, $q_{\max}$ is the maximum phonon wave vector, and L_z is the dimension of the strongest confinement. In our case, $L_z=5$ nm and $c_s=5150$ m s^{-1} in GaAs, then the maximum phonon energy is about 4.3 meV. In Fig. 2(b), the determined rise times increase as the excitation energy is increased: we find 75, 193, and 222 ps for excitations *a*, *b*, and *c*, respectively. These results are consistent with the threshold energy obtained in Eq. (4). Indeed, excitation *a* (5.3 meV) is the closest to $E_{\max}$, and gives the fastest relaxation time; for excitations *b* and *c*, the relaxation rate with emission of one LA phonon is reduced, and the relaxation times are longer. Multiphonon assisted relaxation is commonly admitted to be a possible mechanism for efficient relaxation.[30,31]

In the following, we propose to discuss the dependence of the scattering rate with energy separation between levels in a single QB. Figure 5 shows the relaxation rates $1/\tau_{\text{rel}}$ determined experimentally for QB's with different lengths, as a function of the energy separation between the detection and the excitation energy position. Here, for each QB, the excitation is resonant with the first excited level. We observe that the experimental values present a pronounced maximum for an energy spacing of about 4 meV, and decrease elsewhere. The curve in full line represents the calculated electron–LA-

phonon relaxation rate. The calculation was performed using the Fermi golden rule, which gives the transition probability between two discrete levels:

$$\frac{1}{\tau_{if}} = \frac{2\pi}{\hbar} \sum_q |\langle \Psi_i | W | \Psi_f \rangle|^2 \delta(E_f - E_i + \hbar\omega_q) \qquad (5)$$

for phonon emission of energy $\hbar\omega_q$ at zero temperature. W is the electron-phonon interaction potential, which is equal, for the LA-phonon mode, to: $W = D\sqrt{(\hbar q/2\rho c_s V)} e^{i\vec{q}\cdot\vec{r}}$. V is the volume of the system, ρ is the density of the material, D the deformation potential, and c_s the sound velocity in the material (we took $\rho = 5.36$ g/cm^3, $c_s = 5150$ m s^{-1} for GaAs, and $D = 6.8$ eV). In Eq. (5), Ψ_i and Ψ_f are the electronic wave functions in the initial and final states of energy E_i and E_f, respectively. In order to calculate the wave functions, a separable QWR confining potential was used. In the growth direction we assumed an infinite square well potential of 5-nm width; the thickness variation of the GaAs layer in the lateral direction can be easily represented by a parabolic potential.[18] In these two directions the confinement potential was assumed to be the same for all the QB's. Along the wire axis, small geometry fluctuations create local potential minima that localize the excitons. In this last direction the localization potential is different for each emitting QB, and a parabolic potential with different curvatures was used to represent these fluctuations. The induced confinement is weak, leading to the small level splittings observed in the μPLE spectra. The assumption of a completely separable potential is necessary for the analytical calculation of expression (5). Then the total electronic wave function is simply the product of the separable wave functions. Since the confinement potential along the wire axis is weak (9 meV), the confinement energy of electrons due to localization is more important than for holes. The relaxation of holes is very efficient through their dense spectrum of states. Therefore, we consider that electrons are mainly responsible for the slowing down of relaxation, and we calculate solely the electron–LA-phonon relaxation rate. Nevertheless, an accurate description of phonon scattering should include excitonic effects,[35] and take into account a more precise representation of the confinement potential. This last point is, however, very difficult to obtain because of the complex geometry of the structure.

The calculation shows that the relaxation rate between the first excited and the fundamental state increases as the level spacing $(E_f - E_i)$ increases, reaches a maximum at 4 meV and then decreases again. The maximum value corresponds to the threshold phonon energy deduced in Eq. (4), is well confirmed by the experimental results, and demonstrates that efficient relaxation with the LA phonon depends mostly on the strongest confinement potential. The order of magnitude of the calculated scattering rate is in agreement with the experimental values, showing that the approximate description of the potential is finally quite justified, and that electrons are mainly responsible for the decrease of relaxation. However, it should be pointed out that an important dispersion of the experimental values appears. This might be due to a disorder in the shape of the boxes along the wire direction, which is not well defined and could influence the relaxation rate. Although calculations predict that the relaxation rate should become negligible as the energy spacing is greater than 8 meV, the measured relaxation times remain relatively fast (less than 100 ps). This means that relaxation is still efficient even for an important energy separation between the levels. As an explanation we could consider the presence of optically inactive exciton states between two optically allowed states, as intermediate levels helping in relaxation,[29] or the Auger-like scattering mechanism inside one electron-hole pair proposed in Ref. 32 which finally suppresses the phonon bottleneck.

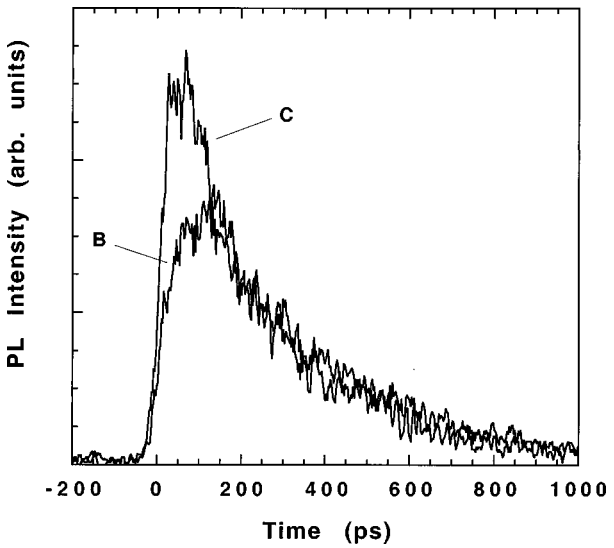

FIG. 6. Time-resolved μPL spectra for resonant excitations *B* and *C* corresponding to the μPLE peaks shown in Fig. 1. The detection energy is the same as position *A* (1.6436 eV).

Another interesting effect observed experimentally and confirmed by the calculation is that relaxation from higher excited states to the fundamental can be more efficient than relaxation from the first excited to the ground state. This is shown in Fig. 6, where two time-resolved spectra of the same QB excited resonantly on the first (spectrum *B*) and second (spectrum *C*) excited levels are represented. These levels correspond to the peaks labeled *B* and *C* on the μPLE spectrum in Fig. 1. Both time-resolved spectra have the same exponential decay connected to the radiative lifetime of the fundamental state. However the rise time is sensitively different in the two experiments. Indeed, values of 50 and 20 ps were found for spectra *B* and *C*, respectively. This clearly indicates that relaxation from the second excited level to the fundamental is more efficient, and the energy separation is the determinant factor acting on the transition rates. Although the wave functions are different for the first and second excited levels, calculations[55] show that the corresponding relaxation rates have a similar dependence with energy separation; that is, they increase until the energy reaches 4 meV, and then decrease again. Therefore the relaxation rate corresponding to *B* will be smaller than *C*, since excitation energy *B* is lower than *C*, leading to a faster relaxation time in the case of excitation *C*.

IV. CONCLUSION

In summary, time and spatially resolved photoluminescence experiments allowed us to determine the radiative life-

time of excitons in single QB's with different lengths formed naturally along the axis of a V-shaped QWR. The confinement potential in this direction is weak (9 meV) and the lengths of the boxes vary from 20 to 100 nm. The radiative lifetimes of the localized excitons are long, ranging from 300 to 500 ps, in comparison with the radiative lifetime of an exciton in a single QWR (150 ps). The radiative recombination rate is found to be proportional to the coherence volume of excitons in the boxes. Resonant relaxation with emission of a LA phonon has been studied as a function of the energy separation between the QB discrete levels. The scattering rate presents a pronounced maximum at 4 meV, corresponding to the threshold phonon energy taking part in the relaxation, as expected theoretically. Relaxation processes remain fast ($<$100 ps), even for higher-energy separation, suggesting that no phonon bottleneck occurs in the present QB's.

[1] P. M. Petroff, A. C. Gossard, and W. Wiegmann, Appl. Phys. Lett. **45**, 620 (1984).

[2] R. Bhat, E. Kapon, D. W. Hwang, M. A. Koza, and C. P. Yun, J. Cryst. Growth **93**, 850 (1988).

[3] B. Etienne, F. Laruelle, Z. Wang, L. Sfaxi, F. Lelarge, F. Petit, T. Mélin, and A. Cavanna, Semicond. Sci. Technol. **11**, 1534 (1996).

[4] E. Kapon, D. W. Hwang, and R. Bhat, Phys. Rev. Lett. **63**, 430 (1989).

[5] X. L. Wang, M. Ogura, and H. Matsuhata, Appl. Phys. Lett. **67**, 804 (1995); **67**, 3629 (1995); Jpn. J. Appl. Phys. **36**, 523 (1997).

[6] A. Gustafsson, F. Reinhardt, G. Biasol, and E. Kapon, Appl. Phys. Lett. **67**, 3673 (1995).

[7] W. Wegscheider, L. N. Pfeiffer, M. M. Dignam, A. Pinczuck, K. W. West, S. L. McCall, and R. Hull, Phys. Rev. Lett. **71**, 4071 (1993).

[8] H. Akiyama, T. Someya, and H. Sakaki, Phys. Rev. B **53**, R16 160 (1996).

[9] See, for example, P. Castrillo, D. Hessman, M.-E. Pistol, S. Anaud, N. Carlsson, W. Seifert, and L. Samuelson, Appl. Phys. Lett. **67**, 1905 (1995).

[10] See, for example, S. Raymond, S. Fafard, P. J. Poole, A. Wojs, P. Hawrylak, C. Gould, A. Sachradja, S. Charbonneau, D. Leonard, R. Leon, P. M. Petroff, and J. L. Merz, Superlattices Microstruct. **21**, 541 (1997), and references therein.

[11] See, for example, Y. Nagamune, H. Watabe, M. Nishioka, and Y. Arakawa, Appl. Phys. Lett. **67**, 3257 (1995).

[12] See, for example, M. Grundmann *et al.*, Phys. Rev. Lett. **74**, 4043 (1995).

[13] R. Grousson, V. Voliotis, N. Grandjean, J. Massies, M. Leroux, and C. Deparis, Phys. Rev. B **55**, 5253 (1997).

[14] A. Zrenner, L. V. Butov, M. Hagn, G. Abstreiter, G. Böhm, and G. Wiegmann, Phys. Rev. Lett. **72**, 3382 (1994).

[15] K. Brunner, G. Abstreiter, G. Böhm, G. Tränkle, and G. Wiegmann, Appl. Phys. Lett. **64**, 3320 (1994).

[16] D. Gammon, E. S. Snow, and D. S. Katzer, Appl. Phys. Lett. **67**, 2391 (1995).

[17] J. Y. Marzin, J. M. Gérard, A. Izraël, D. Barrier, and G. Bastard, Phys. Rev. Lett. **73**, 716 (1994).

[18] J. Bellessa, V. Voliotis, R. Grousson, X. L. Wang, M. Ogura, and H. Matsuhata, Appl. Phys. Lett. **71**, 2481 (1997).

[19] F. Vouilloz, D. Y. Oberli, S. Wiesendanger, B. Dwir, F. Reinhardt, and E. Kapon, Phys. Status Solidi A **164**, 259 (1997).

[20] J. Hasen, L. N. Pfeiffer, A. Pinczuk, S. He, K. W. West, and B. S. Dennis, Nature (London) **390**, 54 (1997).

[21] H. Benisty, C. M. Sotomayor-Torres, and C. Weisbuch, Phys. Rev. B **44**, 10 945 (1991).

[22] U. Bockelmann and G. Bastard, Phys. Rev. B **42**, 8947 (1990).

[23] B. Ohnesorge, M. Albrecht, J. Oshinowo, A. Forchel, and Y. Arakawa, Phys. Rev. B **54**, 11 532 (1996).

[24] U. Bockelmann, W. Heller, A. Filoramo, and P. Roussignol, Phys. Rev. B **55**, 4456 (1997).

[25] S. Raymond, S. Fafard, S. Charbonneau, R. Leon, D. Leonard, P. M. Petroff, and J. L. Merz, Phys. Rev. B **52**, 17 238 (1995).

[26] S. Grosse, J. H. H. Sandmann, G. von Plessen, J. Feldmann, H. Lipsanen, M. Sopanen, J. Tulkki, and J. Ahopelto, Phys. Rev. B **55**, 4473 (1997).

[27] T. H. Gfroerer, M. D. Sturge, K. Kash, J. A. Yater, A. S. Plaut, P. S. D. Lin, L. T. Florez, J. P. Harbison, S. R. Das, and L. Lebrun, Phys. Rev. B **53**, 16 474 (1996).

[28] S. Fafard, R. Leon, D. Leonard, J. L. Merz, and P. M. Petroff, Phys. Rev. B **52**, 5752 (1995).

[29] U. Bockelmann, P. Roussignol, A. Filorame, W. Heller, G. Abstreiter, K. Brunner, G. Böhm, and G. Wiemann, Phys. Rev. Lett. **76**, 3622 (1996).

[30] T. Inoshita, and H. Sakaki, Phys. Rev. B **46**, 7260 (1992).

[31] R. Heitz, M. Grundmann, N. N. Ledentsov, L. Eckey, M. Veit, D. Bimberg, V. M. Ustinov, A. Yu. Egorov, A. E. Zhukov, P. S. Kop'ev, and Zh. I. Alferov, Appl. Phys. Lett. **68**, 361 (1996).

[32] Al. L. Efros, V. A. Kharchenko, and M. Rosen, Solid State Commun. **93**, 281 (1995).

[33] J. Bellessa, V. Voliotis, R. Grousson, X. L. Wang, M. Ogura, and H. Matsuhata, Phys. Status Solidi A **164**, 273 (1997).

[34] N. Notomi, T. Furuta, J. Temmyo, and T. Tamamura, in *Proceedings of the 23rd International Conference on the Physics of Semiconductors, Berlin, 1996*, edited by M. Scheffler and R. Zimmermann (World Scientific, Singapore 1996), Vol. 2, p. 1381.

[35] U. Bockelmann, Phys. Rev. B **48**, 17 637 (1993).

[36] H. Benisty, Phys. Rev. B **51**, 13 281 (1995).

[37] X. L. Wang, M. Ogura, H. Matsuhata, and A. Hamoudi, Appl. Phys. Lett. **71**, 2130 (1997).

[38] G. Bastard, *Wave Mechanics Applied to Semiconductor Heterostructures* (Les Editions de Physique, Les Ulis, 1988).

[39] D. S. Citrin, Superlattices Microstruct. **13**, 303 (1993).

[40] H. Gotoh, H. Ando, and T. Takagahara, J. Appl. Phys. **81**, 1785 (1997).

[41] J. Bellessa, V. Voliotis, R. Grousson, X. L. Wang, M. Ogura, and H. Matsuhata, Solid-State Electron. **42**, 1217 (1998).

[42] E. Blackwood, M. J. Snelling, R. T. Harley, S. R. Andrews, and C. T. B. Foxon, Phys. Rev. B **50**, 14 246 (1994).

[43] D. S. Citrin, Phys. Rev. Lett. **69**, 3393 (1992).

[44] K. Komori, F. Sasaki, X. L. Wang, M. Ogura, and H. Matsuhata, Solid-State Electron **42**, 1211 (1998).

[45] H. Akiyama, S. Koshiba, T. Someya, K. Wada, H. Noge, Y. Nakamura, T. Inoshita, A. Shimizu, and H. Sakaki, Phys. Rev. Lett. **72**, 924 (1994).

[46] E. T. Rashba and G. E. Gurgenishvili, Fiz. Tverd. Tela (Leningrad) **4**, 1029 (1962) [Sov. Phys. Solid State **4**, 759 (1962)].
[47] C. H. Henry and K. Nassau, Phys. Rev. B **1**, 1628 (1970).
[48] T. Takagahara and E. Hanamura, Phys. Rev. Lett. **56**, 2533 (1986).
[49] D. L. Dexter, in *Solid State Physics*, edited by F. Seitz and D. Turnbull (Academic, New York, 1958), Vol. 6, p. 353.
[50] J. Feldmann, G. Peter, E. O. Göbel, P. Dawson, K. Moore, C. Foxon, and R. J. Elliott, Phys. Rev. Lett. **59**, 2337 (1987).
[51] T. Itoh, M. Furumiya, T. Ikehara, and C. Gourdon, Solid State Commun. **73**, 271 (1990).
[52] Y. Kayanuma, Phys. Rev. B **38**, 9797 (1988).
[53] V. Voliotis, R. Grousson, P. Lavallard, and R. Planel, Phys. Rev. B **52**, 10 725 (1995).
[54] M. Bayer, S. N. Walck, T. L. Reinecke, and A. Forchel, Phys. Rev. B **57**, 6584 (1998).
[55] For the sake of simplicity, here we do not present the calculation of the electron–LA-phonon scattering rate for the second excited level.